PRE-PRINT ARTICLE

COPYRIGHT BY COMPOSITES THEORY AND PRACTICE JOURNAL

ISSN: 2299-128X

The influence of plasma spraying parameters on structure and properties of Stellite 31-Cr_3C_2 composite coating

Tadeusz Kubaszek, Barbara Kościelniak, Marek Góral*, Kacper Hładun, Kamila Świerk

Research and Development Laboratory for Aerospace Materials, Rzeszow University of Technology, Powstanców Warszawy 12, 35-959 Rzeszów Poland

Corresponding author e-mail: mgoral@prz.edu.pl

https://doi.org/10.62753/ctp.2024.03.3.3

Abstract

This paper presents the results of a study on the influence of the plasma spraying parameters of a Stellite 31-Cr_2C_3 composite powder containing 30 wt% carbide. The torch current and hydrogen flow rate were taken as variables that affect the energy of the plasma plume. The thickness, porosity and chemical composition of the coating were investigated. Erosion and wear resistance tests in addition to hardness measurements were also carried out. No clear relationships between the spray parameters and the coating properties were found during the study. The coating had a thickness of 200-300 μm, a porosity of 7-12 vol.% and a hardness of approx. 300 HV02.

Introduction

Increasing the durability of machine parts and equipment is determined by the use of materials with high resistance to abrasion and tribological wear. For many years, alloys based on among others cobalt and chromium, known as stellites, have been used for this purpose. These alloys are characterized by high wear [1] and oxidation resistance [2]. In the literature, data on these alloys date back to the 1970s. [3,4]. For many years, stellite coatings have been produced by arc welding [5] laser cladding [6], electrospark deposition [7], plasma transfer arc welding (PTA) [8] as well as detonation spraying [9]. Two methods of thermal spraying

PRE-PRINT ARTICLE
COPYRIGHT BY COMPOSITES THEORY AND PRACTICE JOURNAL
ISSN: 2299-128X

are also often used: HVOF [10] and atmospheric plasma spraying (APS) [11]. The thermal spraying process is often combined with additional processing such as laser remelting [12].

Most of the literature data regards Stellite 6. This coating was sprayed using HVOF[13], D-gun, cold spray [14] and PTA methods. [15]. A wide range of property tests has been carried out for this coating. Jackson et al. investigated the properties of the stellite coating under creep test conditions [16]. Sidhu et al. [17] analysed the hot corrosion of the Stellite 6 alloy used in coal boilers. These alloys are characterized by high oxidation resistance, in many cases higher than MCrAlY coatings [18]. High-temperature corrosion tests were also carried out in molten salts at 900^{o}C [19]. Zhang et al. investigated the cavitation corrosion resistance in a salt solution environment [20]. Kumar et al. [21] studied the solid particle erosion of the Stellite 6 alloy, among others, at 400^{o}C. High-temperature corrosion was also investigated under conditions like those in biomass burning boilers [22].

Various methods have also been developed to modify the Stellite 6 alloy, e.g. by strengthening with titanium carbide particles [23]. The alloy with the addition of lanthanum oxide was also researched, which increased the hardness of the alloy by 1.31 times [24]. The introduction of tungsten carbide allows improved fracture toughness of Stellite 6 [25]. The resistance to fatigue cracking can be raised by introducing nickel or titanium [26].

Few publications deal with the Stellite 31 type alloy. Lucetta et al. [27] used cold spray technology to spray this material including 316L stainless steel. The properties of the coatings indicated that they could be used in the manufacture of plastic parts for the automotive industry. Kharam A. [28] produced a Stellite 31 coating on an Inconel 713LC alloy. The coating was characterised by the presence of chromium and tungsten carbides, resulting in increased hardness up to 482 HV.

Experimental procedure

S235 grade steel was used as the substrate material for the coating spraying processes, from which 40x50x4 mm and 25x50x4 mm samples were cut. A mixture of Oerlikon's cobalt-based METCO 45CNS powder (similar to the Stellite 31 alloy) – the matrix, with the addition of chromium carbide Cr_3C_2 – Metco 70CNS powder, was adopted as the coating material. The proportions used were: 1050 g of matrix powder and 450 g of ceramic additive, accounting

PRE-PRINT ARTICLE
COPYRIGHT BY COMPOSITES THEORY AND PRACTICE JOURNAL
ISSN: 2299-128X

for 30 wt% of the total weight of the mixed powder. For homogenization, the powders were mixed together by means of ball milling for about 8h.

The atmospheric pressure plasma spraying (APS) process was conducted using 5 different sets of parameters (Table 1). The plasma spraying system in the Aerospace Materials Research Laboratory of Rzeszow University of Technology utilising an A60 plasma torch (Thermico, Germany) was used in the experiments. Two variable parameters were changed during test: the hydrogen flow (samples marked H- and H+) as well as the power current (samples marked I- and I+). In each series of the spraying processes, 5 specimens for the different tests were made.

Table 1. Experimental plasma spraying parameters

Sample description	Plasma gasses flow rate, NLPM		Power current, A	Electric power, kW
	Ar	H_2		
S	66	8	500	30.4
H-	70	4	500	27.4
H+	62	12	500	32.7
I-	66	8	300	24.5
I+	66	8	700	40.1

The thickness and porosity of the produced coatings was measured using a Leica 3000 DM light microscope. Image binarization was performed by means of Metilo software. Porosity measurement was then carried out employing Leica Application Suite v3.7. The thickness was measured in three areas of a given sample, with 5 thickness measurements each. The mean value and standard deviation were then calculated. A detailed study of the microstructure of the composite coatings was conducted using a Phenom XL scanning electron microscope (SEM) with a backscattered electron (BSE) detector. The chemical composition and surface distribution of elements were measured by means of a Phenom XL scanning electron microscope equipped with an X-ray energy dispersive detector (EDS) and utilising Phenom-World-PC software.

The erosion resistance test was performed according to ASTM G73 using a Koehler TR-470 at room temperature (25°C). Specimens for the erosion test were cut to 20x20 mm in size. The

PRE-PRINT ARTICLE
COPYRIGHT BY COMPOSITES THEORY AND PRACTICE JOURNAL
ISSN: 2299-128X

duration of the test was 10 minutes. The weight of the specimens before and after the process was determined employing an analytical balance (KERN ABT 120-4M) with an accuracy of 1·10-4 g. The powder flow rate was set at 2 g/min at the air pressure of 0.2 kg/cm^2. The test was performed for specimens placed in the device at a 90° angle to the device nozzle.

Hardness measurements were carried out by means of an Innovatest Nexus 4303 micro-hardness tester, and the Vickers method was used, utilising a diamond indenter with a regular pyramid shape. A force load of 1.96 N and a time of 10 s were applied during the measurements. Five measurements were taken for each coating produced under varying plasma spray conditions.

A Tribotester T-01M device was employed for ball-on-disc wear resistance tests. The conditions were adopted in accordance with the requirements of ASTM G99-17: linear velocity - 0.1 m/s, load 30 N, friction path from 500 m. The friction pair used in the tests was a ball made of WC carbide with a diameter of 10 mm (hardness 1741±5 HV10) and the coating produced by the APS process. The volume loss of the material was calculated from the relationship specified in ASTM G99-17. The width of the abrasion trace was determined by means of a Leica DMI 3000M light microscope and Leica LAS v4.9 image analysis software.

Friction wear resistance was also determined for the produced coatings under varying plasma spray conditions. The test was carried out on the Tribotester T-01M using the ball-on-disc method. The conditions were adopted according to the requirements of ASTM G99-17. The volume loss of the material was calculated from the relationship specified in ASTM G99-17.

$$disk\ volume\ loss = 2\pi \mathrm{R}[r^2 sin^{-1}\left(\frac{d}{2r}\right) - (\frac{d}{4})(4r^2 - d^2)^{\frac{1}{2}}] \qquad (1)$$

Where:

r - radius of the ball [mm]

R - radius of the trace [mm]

d - width of the trace [mm].

PRE-PRINT ARTICLE
COPYRIGHT BY COMPOSITES THEORY AND PRACTICE JOURNAL
ISSN: 2299-128X

Results

Thickness and porosity

In the first stage of the study, the effect of the parameters on the coating thickness was determined. The results show that changing the current and hydrogen intensity affects the thickness of the coating. The highest thickness – 306.78 µm was found for the coating produced at the higher intensity of hydrogen H+. The smallest thickness – 170.23 µm was measured for the coating produced at the lower intensity of hydrogen H- (Fig. 1). Additionally the increasing the power current (I+) resulted in a decrease in the coating thickness to about 212 µm. The thickness of the coating formed using the higher power current (I+) was about 300 µm. The results showed that the power current and hydrogen intensity also affect the amount of porosity. The lowest porosity – 5.5 vol.% was found in the sample produced at the higher hydrogen intensity H+. The highest porosity - 18.92 vol.% was measured for the sample produced under standard S conditions (Table 1, Fig. 2). The changes in power current resulted in decreases in porosity to about 7-8 vol.%.

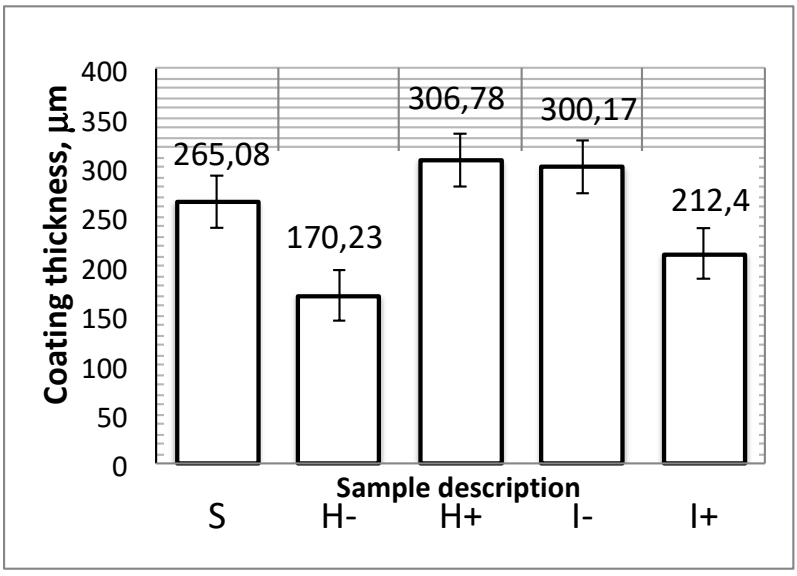

Fig. 1. Thickness of Stellite 31-Cr_2C_3 coatings formed using different spraying parameters (Table 1)

PRE-PRINT ARTICLE
COPYRIGHT BY COMPOSITES THEORY AND PRACTICE JOURNAL
ISSN: 2299-128X

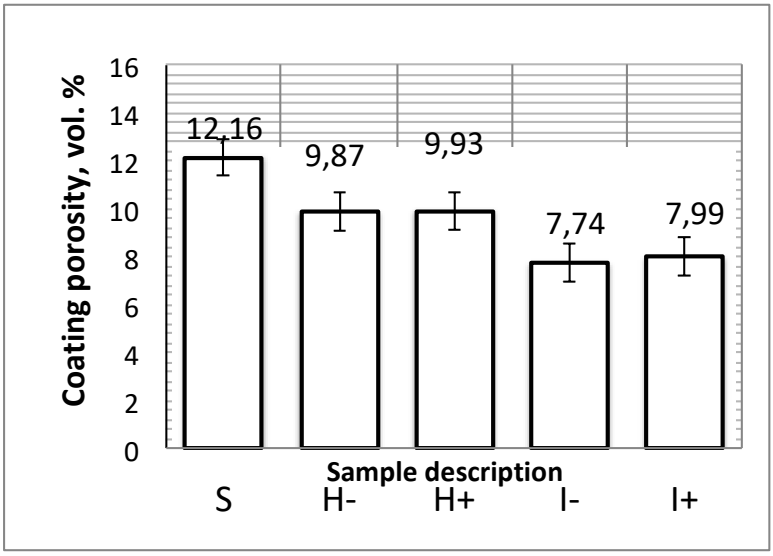

Fig. 2. Porosity of Stellite 31-Cr_2C_3 coatings formed using different spraying parameters (Table 1)

Chemical composition

Elemental mapping was conducted on the coating obtained with standard spray parameters (S, Table 1). Iron was found to be present in the substrate area, while the coating area was dominated by cobalt, nickel and chromium – components of the Stellite 31 alloy (Fig. 3a-f). The uneven distribution of Cr in the coating was due to the concentration of this element in the carbide areas (Fig 3d). This indicates that its distribution is not uniform across the entire coating. The presence of oxygen in some areas indicates partial oxidation of the coating components (Fig. 3e). Analysis of the chemical composition in the microareas showed a similar trend – an even distribution of Co and Ni with an uneven distribution of Cr and the presence of oxygen (Fig 4a-e).

PRE-PRINT ARTICLE

COPYRIGHT BY COMPOSITES THEORY AND PRACTICE JOURNAL

ISSN: 2299-128X

Polish Society of Composite Materials

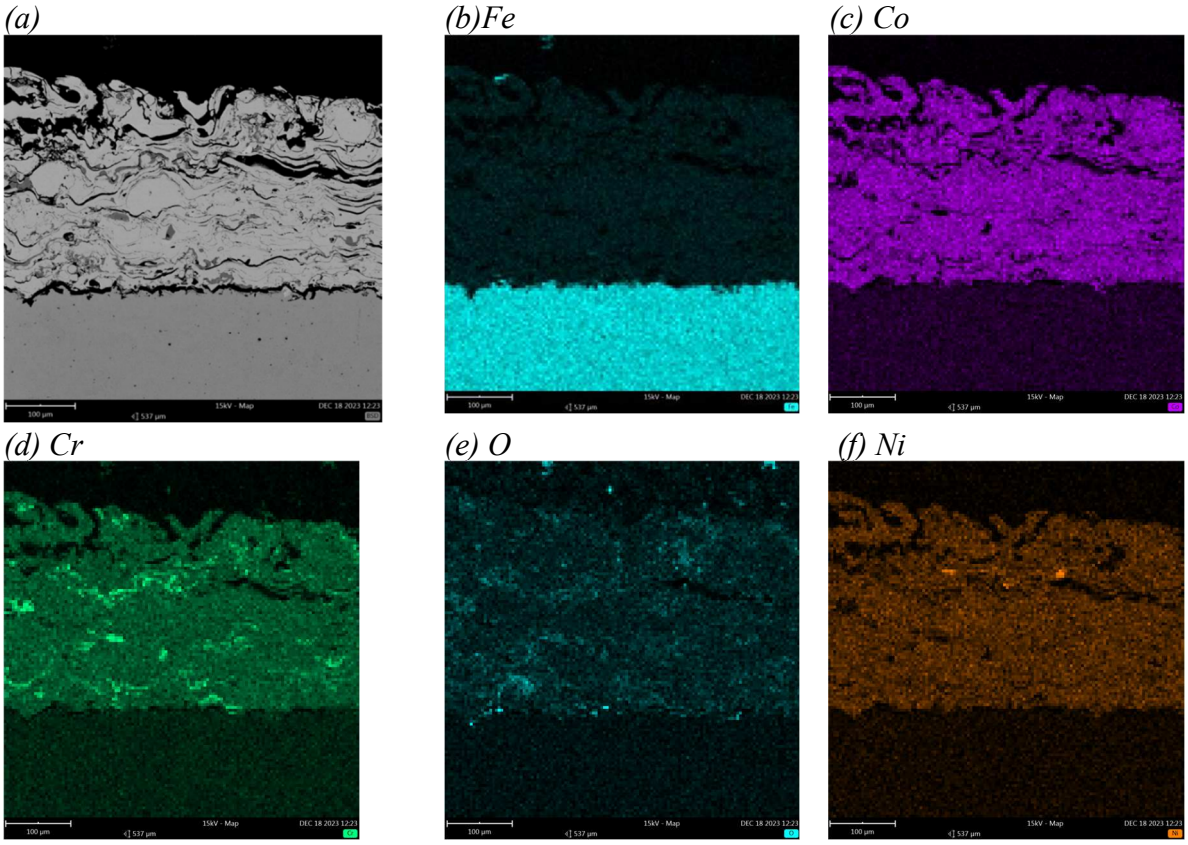

Fig. 3. Microstructure (a) and distribution of b) Fe, c) Co, d) Cr, e) O and f) Ni in cross-section of Stellite 31-Cr_2C_3 coating obtained using standard parameters (S, Table 1)

PRE-PRINT ARTICLE

COPYRIGHT BY COMPOSITES THEORY AND PRACTICE JOURNAL

ISSN: 2299-128X

Polish Society of Composite Materials

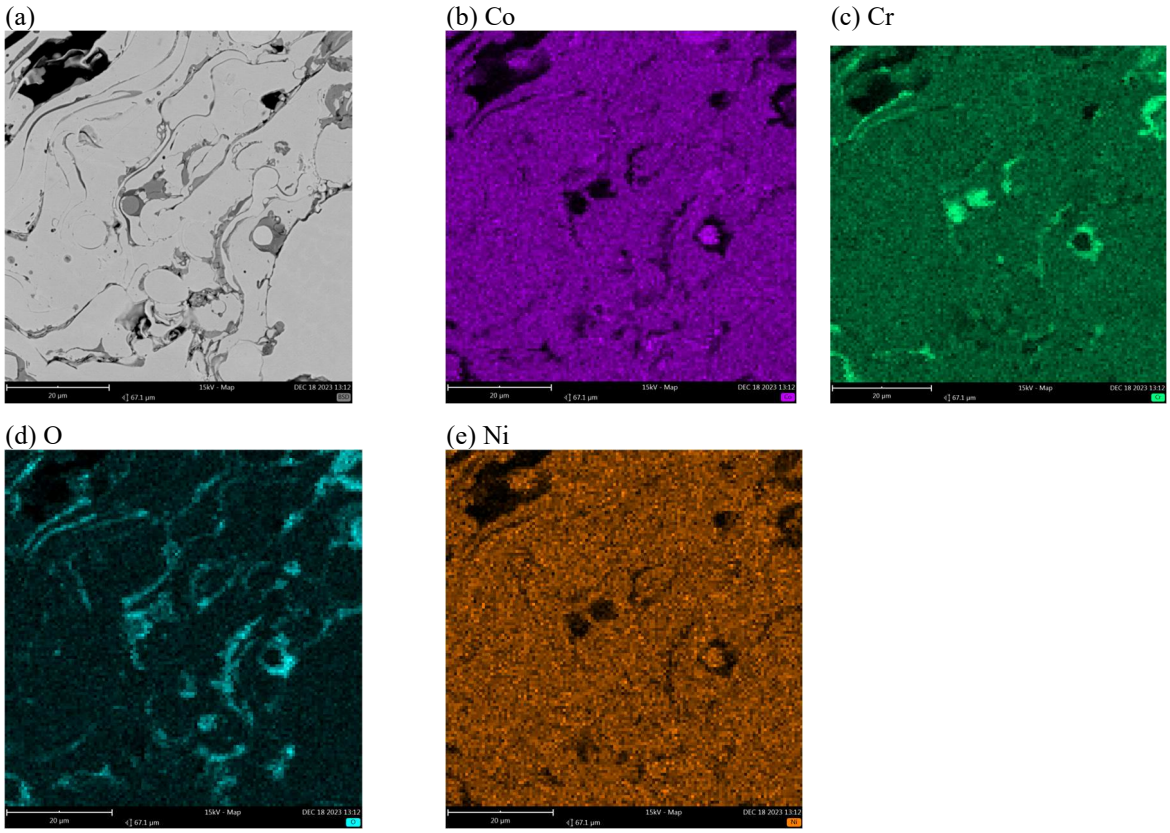

Fig. 4. Microstructure (a) and distribution of b) Co, c) Cr, d) O and e) Ni in microareas of Stellite 31-Cr_3C_2 coating obtained using standard parameters (S, Table 1)

Erosion resistance

For the erosion resistance test, two samples with a manufactured coating of 25x50x4 were used from each spraying run, which were cut to 25x25x4 to fit the Koehler TR-470 machine holder. Three specimens were used in the study. The weight of all the specimens was measured at the beginning of the test and after 10 minutes. It the case of the influence of the hydrogen flow rate, it was found that the best erosion resistance was characterized by the coating with the lowest hydrogen flow rate (H-) (Fig. 5). The determined weight loss for this coating was 5.03×10^{-3} g. It was also found that increasing the hydrogen flow (H+) rate in the plasma gas mixture raised the coating's weight loss after erosion testing by 3×10^{-4} and 7×10^{-4} g at hydrogen flow rates of 8 (-) and 12 NLPM (H+), respectively. The second of the investigated plasma spraying conditions was the power current (Fig. 5). An inverse relationship of weight loss with respect to increasing current intensity was observed. The best erosion resistance, and therefore the smallest weight loss, was exhibited by the coating deposited with the highest current intensity (I+). The smallest weight loss of all the studied

PRE-PRINT ARTICLE
COPYRIGHT BY COMPOSITES THEORY AND PRACTICE JOURNAL
ISSN: 2299-128X

specimens was determined for this coating and it was $4.55x10^{-3}$ g. The use of lower current intensities of 300 (I-) and 500 A (S) in the APS spraying process resulted in a coating weight loss of about $5.2x10^{-3}$ g.

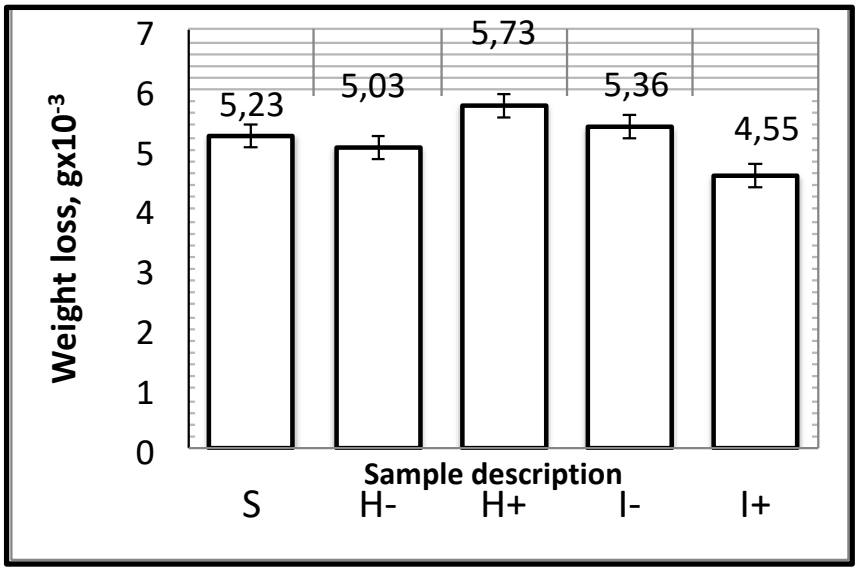

Fig. 5. Total weight loss during erosion test of Stellite 31-CrC coating deposited using different spraying parameters (Table 1)

Hardness of coatings

Based on the conducted tests, a similar effect of the applied hydrogen flow rate on the hardness of the obtained coatings was observed as in the case of erosion resistance (Figure 5). The highest hardness was obtained for the coating produced at the lowest hydrogen flow rate (H-) amounting to 382.25 HV0.2. It was found that increasing the hydrogen flow rate affects the obtained values by about 100 HV0.2 at the H_2 flow rate of 8 NLPM (S) and by about 30 HV0.2 at the H_2 flow rate of 12 NLPM (H+). A similar dependence of power current on hardness regarding the specified erosion resistance was also observed (Fig. 6). The highest hardness was obtained by the coating with the increased current intensity of 700A (I+) equal to 335.05 HV0.2. The use of lower power current intensities of 300 (I-) and 500 A (S) resulted in a similar hardness of about 270 HV0.2.

PRE-PRINT ARTICLE
COPYRIGHT BY COMPOSITES THEORY AND PRACTICE JOURNAL
ISSN: 2299-128X

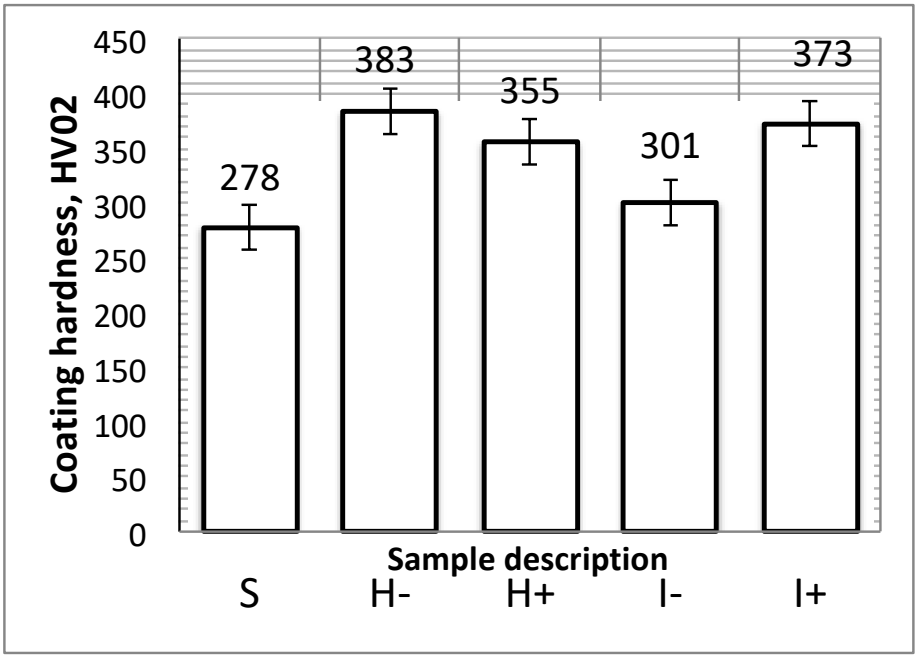

Fig. 6. Hardness measurement results of Stellite 31-CrC coating deposited using different spraying parameters (Table 1)

Wear resistance – pin-on-disk test

Wear resistance tests under frictional conditions showed the highest volume loss of the coating when the flow of hydrogen was reduced to 4 NLPM (H-), which amounted to 4.2 $x10^{-3}$ mm^3. It was also shown that increasing the flow rate of hydrogen in the plasma gas mixture produced coatings with higher wear resistance – the specific volume loss was $3.3x10^{-3}$ mm^3 and 3.6 $x10^{-3}$ mm^3 for the coatings at hydrogen flow rates of 8 (S) and 12 NLPM (H+), respectively. For the second spraying condition tested – power current – the smallest volume loss was found for the coatings at the highest (700A, I+) and lowest (300A, I-) power current. It amounted to 2.9 $x10^{-3}$ mm^3. The average value of power current resulted in the coating with the highest volume loss – 3.3 $x10^{-3}$ mm^3, and thus the worst friction wear resistance.

PRE-PRINT ARTICLE
COPYRIGHT BY COMPOSITES THEORY AND PRACTICE JOURNAL
ISSN: 2299-128X

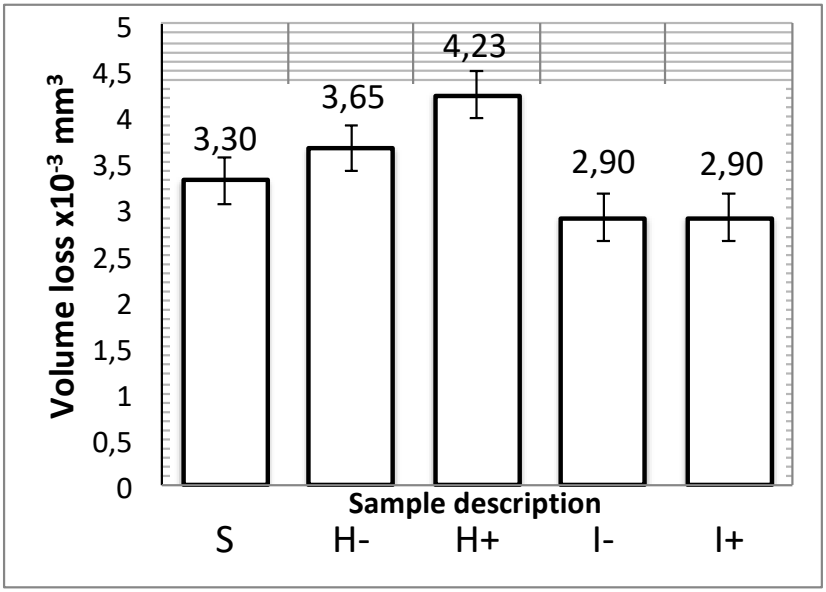

Fig. 7. Total volume loss during pin-on-disk test of Stellite 31-CrC coating deposited using different spraying parameters (Table 1)

Discussion

The conducted research was designed to examine the feasibility of a composite coating composed of Stellite 31 alloy with an addition of 30 wt% chromium carbide. The powders were self-mixed in a ball mill (without additional balls), which should not alter the grain size of the individual components. A very wide range of current and hydrogen flow rates was chosen in the experimental plan (Table 1). The results of the thickness measurements did not allow the influence of the individual changed parameters on it to be clearly established in comparison with previously investigated cermet coatings [28]. However, it was found that changes in the current intensity resulted in a decrease in porosity to about 7-8 vol.% and in hydrogen intensity to about 9-10 vol.%, compared to 12 vol.% for the standard conditions (S). Nevertheless, analysis of the chemical composition on the cross-section of the coating showed an uneven distribution of chromium in the matrix where chromium carbide was present. This indicates its non-uniform distribution in the coating despite prolonged mixing of the powder before spraying. Partial oxidation of the coating was also observed, as indicated by the presence of oxygen. The results of the erosion test showed that increasing the current to 700A (I+ parameters) reduced the erosion wear below the $5x10^{-3}$g values recorded for the coating sprayed using the other parameters. It is significant that the coating obtained at this amperage

PRE-PRINT ARTICLE
COPYRIGHT BY COMPOSITES THEORY AND PRACTICE JOURNAL
ISSN: 2299-128X

was characterised by one of the highest measured hardness values – 373 HV0.2. In the other cases, the hardness was above 300 HV0.2, except for the coating sprayed using the standard parameters (S, hardness 278 HV0.2).

The change in the current significantly affected the wear of the coating in the pin-on-disk test. The material loss was 2.9 $x10^{-3}mm^3$. The change in the hydrogen intensity resulted in higher wear compared to the coating sprayed at standard conditions (S, $3.3x10^{-3}mm^3$). All the obtained values are several times higher than the results obtained for the Stellite 6 and 12 alloys [29] – about 0.0012 $x10^{-3}mm^3$.

The achieved hardness of the Stellite coatings containing the chromium carbide coating was lower than that measured for the Stellite 31 alloy alone (over 480 HV) and reported by Khorram et. al [30]. This might be connected with a few factors. The high current intensity and the increased amount of hydrogen in the plasma plume resulted in raised heat energy and temperature, which, on the one hand, facilitated melting of the Stellite matrix, and on the other hand, decarburisation of the chromium carbide, which significantly alters the hardness [31]. On the other hand, reducing the plasma energy by decreasing the amount of hydrogen injected or lowering the power current significantly limits the decomposition of the carbide, but on the other hand, limits the melting of the matrix [32, 33]. On the basis of the conducted tests, the influence of individual spraying parameters is ambiguous [34], which is further implied by the uneven distribution of chromium carbide in the matrix in comparison with previously investigated commercial powders [35], and thus the unevenness of the obtained results of porosity, hardness as well as the wear and erosion tests. Owing to the small amount of Cr_3C_2 introduced into the powder (30 wt%) compared to commercial carbide powders, in which its amount can exceed 70 wt% [36], its effect was not significant. This indicates the need to investigate powders with a much higher content of hard ceramic particles [36] and to employ a much harder matrix, e.g. Stellite 6 or 12 alloys [6-16].

References

1. Inman, I.A., Rose, S.R., Datta, P.K., Studies of high temperature sliding wear of metallic dissimilar interfaces II: Incoloy MA956 versus Stellite 6, Tribology International, 39(2006)11, pp. 1361–1375, DOI 10.1016/j.triboint.2005.12.001

PRE-PRINT ARTICLE

COPYRIGHT BY COMPOSITES THEORY AND PRACTICE JOURNAL

ISSN: 2299-128X

2. Sidhu, B.S., Prakash, S., High-temperature oxidation behavior of NiCrA1Y bond coats and stellite-6 plasma-sprayed coatings, Oxidation of Metals, 63 (2005) 3-4, pp. 241–259, DOI 10.1007/s11085-005-3203-1
3. Stott, F.H., Stevenson, C.W., Wood, G.C., Friction and wear properties of Stellite 31 at temperatures from 293 to 1073K, Metals Technology, 4 (1977) 1, pp. 66–74, DOI 10.1179/030716977803292169
4. Edington, J.W., Wright, I.G., Study of particle erosion damage in Haynes Stellite 6B I: Scanning electron microscopy of eroded surfaces, Wear, 48(1978) 1, pp. 131–144, DOI 10.1016/0043-1648(78)90143-6
5. Atamert, S., Bhadeshia, H.K.D.H., Comparison of the microstructures and abrasive wear properties of stellite hardfacing alloys deposited by arc welding and laser cladding, Metallurgical Transactions A, 20 (1989) 6, pp. 1037–1054, DOI 10.1007/BF02650140
6. Giordano, L., Ramous, E., Ferraro, F., Pasquini, F., La Rocca, A.V., Comparison of stellite hardfacing by laser and traditional techniques, High temperature technology, 2(1984)4, pp. 213–216, 1984, DOI 10.1080/02619180.1984.11753265
7. Chen, C.J., Wang, M.C., Wang, D.S., Liang, H.S., Feng, P., Characterisations of electrospark deposition Stellite 6 alloy coating on 316L sealed valve used in nuclear power plant, Materials Science and Technology, 26 (2010) 3, pp. 276–280, DOI 10.1179/174328409X430447
8. Yang, L.J., Loh, N.L., The wear properties of plasma transferred arc cladded stellite specimens, Surface and Coatings Technology, 71 (1995) 2, pp. 196–200, DOI 10.1016/0257-8972(94)01021-A
9. Ningkang, H., Yi, W., Zhong, Z.X., Pu, W.X., Electron beam treatment of detonation-sprayed Stellite coatings, Surface and Coatings Technology, 46 (1991) 3, pp. 255–263, DOI 10.1016/0257-8972(91)90168-V
10. Huang, S.W., Nolan, D., Kusmoko, A., Norrish, J., Dunne, D., A comparative study of Stellite 6 coatings produced by Laser cladding, HVOF and plasma spraying techniques, PICALO 2004 - 1st Pacific International Conference on Applications of Laser and Optics, Conference Proceedings, pp. 7–11, 2004, DOI 10.2351/1.5056090
11. Sidhu, B.S., Prakash, S., Erosion-corrosion of plasma as sprayed and laser remelted Stellite-6 coatings in a coal fired boiler, Wear, 260 (2006) 9-10, pp. 1035–1044, DOI 10.1016/j.wear.2005.07.003
12. Sidhu, B.S., Puri, D., Prakash, S., Mechanical and metallurgical properties of plasma sprayed and laser remelted Ni-20Cr and Stellite-6 coatings, Journal of Materials Processing Technology, 159 (2005) 3, pp. 347–355, DOI 10.1016/j.jmatprotec.2004.05.023,
13. Sassatelli P., Bolelli G., Vippola M., Properties of HVOF-sprayed Stellite-6 coatings, Surface and Coatings Technology, 338 (2018), pp 45-62, https://doi.org/10.1016/j.surfcoat.2018.01.078
14. Rajab A., Seraj A., Abdollah-Z,. Garcia Cano I., Comparison of Stellite coatings on low carbon steel produced by CGS and HVOF spraying, Surface and Coatings Technology, 372 (2019), pp. 299-311, https://doi.org/10.1016/j.surfcoat.2019.05.022
15. Wang R., Ye S. Lu X., Effect of copper oxides on defect formation during PTA cladding of Stellite 6 on copper substrates, Surface and Coatings Technology, 466 (2023), 129625, https://doi.org/10.1016/j.surfcoat.2023.129625

PRE-PRINT ARTICLE

COPYRIGHT BY COMPOSITES THEORY AND PRACTICE JOURNAL

ISSN: 2299-128X

16. Jackson G. A., Bai M., Sun W., Small punch creep testing of thermally sprayed Stellite 6 coating: A comparative study of as-received vs post-heat treatment Materials Science and Engineering: A, 749 (2019), pp. 137-147, https://doi.org/10.1016/j.msea.2019.02.030,
17. Sidhu T.S., Prakash S., Agrawal R. D., Hot corrosion studies of HVOF NiCrBSi and Stellite-6 coatings on a Ni-based superalloy in an actual industrial environment of a coal fired boiler, Surface and Coatings Technology, 201 (2006) 3–4, pp. 1602-1612, https://doi.org/10.1016/j.surfcoat.2006.02.047
18. Singh B., Sidhu T.S. Prakash S., Performance of NiCrAlY, Ni–Cr, Stellite-6 and Ni_3Al coatings in Na2SO4–60% V2O5 environment at 900 °C under cyclic conditions, Surface and Coatings Technology, 201 (2006) 3, pp. 1643-1654 DOI: 10.1016/j.surfcoat.2006.02.035
19. Singh B. Sidhu T.S., Prakash S., Studies on the behavior of stellite-6 as plasma sprayed and laser remelted coatings in molten salt environment at 900°C under cyclic conditions, Surface and Coatings Technology, 201 (2006)3–4, pp. 1643-1654, https://doi.org/10.1016/j.surfcoat.2006.02.035
20. Zhang Q. Wu L. Yao J., Correlation between microstructural characteristics and cavitation resistance of Stellite-6 coatings on 17-4 PH stainless steel prepared with supersonic laser deposition and laser cladding, Journal of Alloys and Compounds, 860 (2021), 158417, https://doi.org/10.1016/j.jallcom.2020.158417
21. Kumar P. Singh S. Mishra B., Studies on solid particle erosion behaviour of D-Gun sprayed WC-Co, Stellite 6 and Stellite 21 coatings on SAE213-T12 boiler steel at 400 °C temperature, Surface and Coatings Technology, 385(2020), 125353, https://doi.org/10.1016/j.surfcoat.2020.125353
22. Chi H., A. Pans M., Liu H., Experimental investigations on the chlorine-induced corrosion of HVOF thermal sprayed Stellite-6 and NiAl coatings with fluidised bed biomass/anthracite combustion systems, Fuel, 288 (2021),119607, https://doi.org/10.1016/j.fuel.2020.119607
23. Shahroozi A., Afsari A., Khalifeh A. R., Microstructure and mechanical properties investigation of stellite 6 and Stellite 6/TiC coating on ASTM A105 steel produced by TIG welding process, Surface and Coatings Technology, 350 (2018), pp 648-658, https://doi.org/10.1016/j.surfcoat.2018.07.044
24. Fang Y. Cui X. Jin G., Influence of La_2O_3 addition on nano indentation hardness and residual stress of Stellite 6 coating prepared by plasma cladding, Journal of Rare Earths Volume 36, 8, (2018), pp 873-878, https://doi.org/10.1016/j.jre.2018.03.008
25. Li Y. Liu X. Ren X., A method to eliminate the cracking of Stellite 6 + WC laser cladding layers using ultrasonic impact treatment, Materials Letters, 355, (2024), 135491, https://doi.org/10.1016/j.matlet.2023.135491
26. Wu Y., Liu Y., Cao X., Developing the ductility and thermal fatigue cracking property of laser-deposited Stellite 6 coatings by adding titanium and nickel, Materials & Design, 162, 15 (2019), pp. 271-284, https://doi.org/10.1016/j.matdes.2018.11.063
27. Lucchetta G., Giusti R., Vezzu S., Bariani P.F., Investigation and characterization of Stellite-based wear-resistant coatings applied to steel moulds by cold-spray, CIRP Annals - Manufacturing Technology, 64 (2015), pp. 535–538, https://doi.org/10.1016/j.cirp.2015.04.031
28. Goral, M., Kubaszek, T., Grabon, W.A., Grochalski, K., Drajewicz, M., The Concept of WC-CrC-Ni Plasma-Sprayed Coating with the Addition of YSZ Nanopowder for

PRE-PRINT ARTICLE

COPYRIGHT BY COMPOSITES THEORY AND PRACTICE JOURNAL

ISSN: 2299-128X

Cylinder Liner Applications, Materials, 2023, 16(3), 1199, DOI 10.3390/ma16031199

29. Liu R., Yao J.H., Zhang Q.L., Yao M.X., Collier R., Sliding wear and solid-particle erosion resistance of a novel high-tungsten Stellite alloy, Wear 322-323 (2015) 41–50, http://dx.doi.org/10.1016/j.wear.2014.10.012
30. Khorram A., Microstructural evolution of laser clad Stellite 31 powder on Inconel 713 LC superalloy, Surface and Coatings Technology, 423 (2021), 127633, https://doi.org/10.1016/j.surfcoat.2021.127633
31. Matthews S., Development of high carbide dissolution/low carbon loss Cr3C2–NiCr coatings by shrouded plasma spraying, Surface and Coatings Technology, 258 (2014), Pp 886-900, https://doi.org/10.1016/j.surfcoat.2014.07.062
32. Kubaszek T., Góral M., Słyś A., Szczęch D, Kancarczyk K., Drajewicz M., The influence of HV-APS process parameters on microstructure and erosion resistance of metalloceramic WC-CrC-Ni coatings, Ceramics International, 49 (2023) 11, Part A, pp. 18007-18013, https://doi.org/10.1016/j.ceramint.2023.02.148
33. Richert M.W., Mikułowski B. , Pałka P., Hotloś A., Perek-Nowak M., The Effect of Chemical Composition and Thermal Sprayed Method on the Chromium and Tungsten Carbides Coatings Microstructure, Journal of Surface Engineered Materials and Advanced Technology, 2013, 3, 1-5, http://dx.doi.org/10.4236/jsemat.2013.31001
34. Thao D.X., Got H. V., Cuong Ph. D., Optimization of Plasma Spraying Parameters with Respect to Shear Adhesion Strength of Cr3C2-NiCr Coating on 16Mn Steel, Tribology in Industry, 44 (2022) 2, pp. 221-229, DOI: 10.24874/ti.1101.04.21.09
35. Szymkiewicz, K., Góral, M., Kubaszek, T., Gancarczyk, K., Effect of plasma spraying parameters on microstructure and thickness and porosity of WC-CrC-Ni coatings deposited on titanium, Kovove Materialy, 2023, 61(4), pp. 223–231, DOI 10.31577/km.2023.4.223
36. Dang T. X., Son N. H., Cuong Ph. D., Research on optimizing spray parameters for Cr_3C_2 – NiCr coating created on alloy steel by plasma spraying technique, Journal of Machine Engineering, 22 (2022) 4, pp. 43–53, https:/doi.org/10.36897/jme/157047